HHS Public Access

Author manuscript

Invest Radiol. Author manuscript; available in PMC 2016 December 01.

Published in final edited form as:

Invest Radiol. 2015 December ; 50(12): 821–827. doi:10.1097/RLI.0000000000000190.

Renal BOLD MRI: A Sensitive and Objective Analysis

Jon M. Thacker, BA[1], **Lu-Ping Li, PhD**[2,4], **Wei Li, MD**[2], **Ying Zhou, PhD**[5], **Stuart M. Sprague, DO**[3,4], and **Pottumarthi V Prasad, PhD**[2,4]

[1]Department of Biomedical Engineering, Northwestern University, Evanston, IL

[2]Department of Radiology / Center for Advanced Imaging, NorthShore University Healthsystem, Evanston, IL

[3]Department of Medicine, NorthShore University Healthsystem Evanston, IL

[4]Department of Medicine, University of Chicago Pritzker School of Medicine, Chicago, IL

[5]Center for Biomedical and Research Informatics, NorthShore University Healthsystem, Evanston, IL

Abstract

Objectives—To determine a robust (sensitive and objective) method for analyzing renal blood oxygenation level-dependent (BOLD) MRI data.

Materials and Methods—47 subjects (30 with Chronic Kidney Disease and 17 controls) were imaged at baseline and following furosemide with a multi-echo gradient recalled echo sequence. Conventional analysis consisted of regional segmentation (small-cortex, large-cortex and medulla), followed by computing the mean of each region. Additionally, we segmented the entire parenchyma and computed the mean (μ_1) plus higher moments (μ_2, μ_3, and μ_4). Two raters performed each of the segmentation steps and agreement was assessed with intra-class correlation coefficients (ICC). We used a measure of effect size (Cohen's *d* value), in addition to the usual measure of statistical significance, *p*-values, for determining significant results.

Results—The mean of the renal parenchyma showed the highest agreement between raters (ICC=0.99), and the higher parenchyma moments were on par with large cortical ROI ICC. The renal parenchymal mean also exhibited significant sensitivity to changes post-furosemide in healthy subjects (p=0.002, d=0.84); in agreement with medullary ROIs (p=0.002, d=1.59). When comparing controls and subjects with CKD at baseline, cortical ROI showed a significant difference (p=0.015, d=−0.69) while the parenchyma ROI did not (p=0.152, d=0.39). Post-furosemide data in all regions resulted in a significant difference (large-cortex: p=0.026, d=−0.51; medulla: p=0.019, d=−0.61) with the renal parenchyma ROI resulting in the largest effect size (p=0.003, d=−0.75). Higher moments of the renal parenchyma showed similar significant differences as well.

Conclusions—Overall, our data support the use of the entire parenchyma to evaluate changes in the medulla following administration of furosemide, a widely used pharmacological maneuver.

Corresponding Author: Pottumarthi V. Prasad, Ph.D., Department of Radiology, Walgreen Building, Suite G507, 2650 Ridge Avenue, Evanston, IL 60201, Tel: (847) 570-1948 pprasad@northshore.org.

Changes in higher moments indicate that there is more than just a shift in the mean renal R2* and may provide clinically relevant information without the need for subjective regional segmentation. For evaluating differences between controls and subjects with CKD at baseline; large cortical ROI provided the highest sensitivity and objectivity. A combination of renal parenchyma assessment and large cortical ROI may provide the most robust method of evaluating renal BOLD MRI data.

Keywords

renal; chronic kidney disease; oxygenation; BOLD MRI; R2* distribution

Introduction

Renal hypoxia is thought to play a key role in the progression of chronic kidney disease (CKD)[1,2], leading to an interest in non-invasive assessment of renal oxygenation. Renal blood oxygenation level-dependent (BOLD) magnetic resonance imaging is currently the only known non-invasive method that can be used to evaluate renal oxygenation in humans[3,4]. Extensive research has shown that this technique has the ability to detect intra-subject changes following various interventions[3,5–7]. There is a growing interest in applying this method to distinguish different groups of subjects, such as those with CKD, as compared to control subjects[8–11]. However, experience to-date has led to conflicting reports on whether renal BOLD can detect differences between controls and subjects with CKD. Non-uniform hydration status between subjects, varied oxygenation due to multiple etiologies and a variation in medication amongst the subjects may at least in part explain some of the discrepancies[12]. Additionally, the method of analysis may play a role[10].

Renal BOLD MRI studies have predominantly used the mean value of small, manually defined ROI within the cortex and medulla. This technique is useful for cases where the renal cortex and medulla are readily discernable, such as at baseline in healthy subjects. However, the contrast may not be sufficient to distinguish the two regions in patients with CKD or even healthy subjects following furosemide administration[7]. It is known that cortico-medullary contrast decreases in advanced CKD, making this technique sub-optimal for analyzing such cases[13]. Recent studies have indicated the subjectivity of this regional segmentation technique and a few methods to overcome the limitations have been proposed[14–16]. There is an inherent heterogeneity in the distribution of R2* values even within each of the two different renal tissues[17]. Researchers have attempted to reduce this variation by defining several ROIs and taking the average of their means as a measure of R2* for each region[18]. Alternately, in the cortex, it is possible to define a large ROI that acts as an average across the entire region.

A method that minimizes the subjectivity of ROI placement in renal BOLD analysis will be especially important for comparing data from different institutions and establishing renal BOLD MRI as a clinically viable technique[19]. One method of addressing these issues is through histogram analysis of the renal parenchyma. Histogram analysis has been effectively applied to diffusion maps in the cervical cord of multiple-sclerosis patients[20], diffusion images for intracranial tumor differentiation[21] and renal tumor classification[22], and more recently to arterial spin labeled images of mild CKD patients[23]. Based on this general

principle, we have tested the hypothesis that a method that analyzes the R2* distribution of the entire renal parenchyma will be able to detect quantitative changes in subjects following interventions and between groups of subjects with different levels of kidney function. Due to the mixed distribution of tissues within the parenchyma when taken as a whole entity, the renal R2* distribution will not be normally distributed. This implies that the mean and standard deviations (first two moments) may not be sufficient to fully represent the actual distribution. We have explored the use of two additional moments for characterizing this distribution. While our method is related to histogram analysis, it does not require a bin size and assumes nothing about the distribution of values. Furthermore, we utilize a kernel density estimate of the empirical distribution when displaying the distributions, as it does not require a bin size as well. Hence forth, our method will be referred to as moment analysis.

To determine a robust (sensitive and objective) method for analyzing renal blood oxygenation level-dependent (BOLD) MRI data, we have evaluated the ability of conventional BOLD analysis and parenchyma moment analysis to detect inter- and intra-subject differences in controls and subjects with CKD. Specifically, we have evaluated the inter-rater agreement, sensitivity to changes following administration of furosemide, and the relative sensitivity of the methods in differentiating controls from subjects with CKD.

Materials and Methods

Subjects

All procedures were performed with approval from the institutional review board and written subject consent. A total of 47 subjects participated: controls (n=17; age: 41.6±12.9 yrs; estimated glomerular filtration rate (eGFR)=97.1±15.0 ml/min/1.73m^2; 9 male/8 female), CKD (age: 61.9±10.4 years; eGFR in the range of 30–90 ml/min/1.73m^2 (n=20) and < 30 ml/min/1.73m^2(n=10); proteinuria = 0.83 ± 0.9; systolic BP=130.7±25.6 mm Hg; diastolic blood pressure=70.7±15.5 mm Hg; avgerage duration = 7.6 ± 5.2 years; 15 male/15 female). Subjects with unilateral disease were excluded. Subjects were instructed to fast starting after midnight on the day of the study. The scanning was performed in the morning.

MRI Protocol

All experiments were performed on a 3 Tesla whole-body scanner (MAGNETOM Verio, Siemens Healthcare, Erlangen, Germany) equipped with high performance gradient coils (45 mT/m maximum gradient strength, 200 mT/m/ms slew rate). A body array coil was used for transmission and the spine and body array coils were combined for signal reception. All subjects were examined in the supine position with their feet entering the scanner first. BOLD MRI data was acquired using a breath-hold multiple gradient echo (mGRE) sequence with following parameters: field of view = 360 × 245mm, number of slices = 5, slice thickness = 5.0mm, matrix size = 256 × 176, repetition time = 62ms, number of echoes = 8 equally spaced (3.09–32.3ms), averages = 1, flip angle = 30°. BOLD MRI measurements were made at baseline. The patient table was moved to administer 20 mg of furosemide *iv*. Post-furosemide data was acquired approximately 15-minutes after the baseline scans. The

action of furosemide is to inhibit reabsorptive transport along the medullary thick ascending limb which increases medullary PO2[24].

R2* Maps

The eight images from each mGRE acquisition were used to estimate R2* on a voxel-by-voxel basis, using an offline linear least squares regression. Magnitude images were thresholded at 20 (a.u.) to remove values where the R2* is so high that the signal decays into the noise floor in later echoes. These occur in places with large changes in susceptibility such as regions neighboring the large intestines or areas of no signal (background). Typically this resulted in less than a mean loss of 7% (0.2% median) voxels within a ROI. R2* maps were created for each subject at baseline, and post-furosemide administration.

Regions of Interest

Two observers defined ROIs in the cortex, medulla, and the entire renal parenchyma for both the left and right kidneys on the first mGRE image of the center slice. Care was taken not to include any voxels from areas near strong susceptibility changes or other artifacts. Tumors and cysts were excluded from the ROIs as well (2 cases). Additionally, macroscopic vasculature was removed when it was readily apparent to the observers. However, they represent a very small number of voxels within the whole parenchyma and are thus expected to have a minimal effect on the computed values, even when not completely removed. Cortical ROIs were drawn according to two common methods: 2–3 small ROIs (<100 voxels) and one large ROI (>500 voxels) encompassing the vast majority of the cortex (Figure 1). Separate ROIs were defined for each subject at baseline and post-furosemide.

After all the ROIs were defined, they were copied to the R2* maps to compute the mean value for each region. ROIs on baseline images were matched to post-furosemide images when possible but were drawn separately. The parenchyma ROI was used for higher moment analysis in a similar fashion.

Moment Analysis

Following manual segmentation of the renal parenchyma, the R2* distributions were analyzed using four sample moments (μ_1, μ_2, μ_3, *and* μ_4). The first moment is the sample mean μ_1, and the next three are central moments (computed around the mean). Given the mean μ_1, for $n > 1$, the n^{th} central moment of an image, I, containing V voxels, is defined as

$$\mu_n = \frac{1}{V}\sum_{i=1}^{V}(I_i - \mu_1)^n .$$

In statistics, the first three moments after the sample mean are commonly referred to as the standard deviation (μ_2), skewness (μ_3) and kurtosis (μ_4). These can be considered to describe the shape features of the distribution. These names generally refer to standardized moments, which are defined in relation to the normal distribution. The parenchyma distribution is not expected to be normally distributed due to the inclusion of two distinct regional distributions, we preferred to use the actual moments as parameters rather than use the standard statistical nomenclature.

These methods reduce the large number of R2* parenchyma samples to a set of numerical values summarizing the shape of the distribution. Thus, each subject had four values per stage (baseline and post-furosemide). Statistical comparisons were performed with this set of data.

Statistical Analysis

Statistically significant changes were assessed between baseline and post-furosemide R2* measurements, separately in control and CKD groups, for each of the regions. A Wilcoxon non-parametric test was used for this matched pairs comparison. Control and CKD groups were compared in each region and at each stage for statistically significant differences with a Mann-Whitney U test. To help estimate the effect size for each comparison, we report Cohen's d. The use of effect size in addition to p values has been recommended for scientific reporting[25]. Cohen's d effectively represents the effect size in three levels: small, medium and large corresponding to d values greater than or equal to 0.2, 0.5 and 0.8 respectively. We report values as being *pragmatically significant* when there is both a substantial effect size, (*i.e.* $|d| \geq 0.5$) and *statistical significance* (*i.e.* $p < 0.05$). Multiple comparisons were corrected for by applying the Holm-Bonferroni method to limit the family wise error rate in reporting false rejections of the null hypothesis. This correction was applied to each set of regional measurements. Values are reported as the mean ± standard deviation where applicable. All analysis was performed using Python 2.7.2 and the SciPy 0.13.3 module[26].

To assess the effects of variability in the definition of ROIs on the computed values, the intra-class correlation coefficients (ICC) were evaluated. The ICC will be high when there is little variation between the scores given to each subject by the raters. ICC values are generally stratified as poor agreement (<0.75), moderate agreement (>0.75) and good agreement (>0.9). ICCs were determined for the mean value of each region and between the various measures used in the multiple moment method.

Results

Comparison of Mean Values

Figure 1 shows an example of these ROIs and the potential variation in the mean values of the individual ROIs. The mean R2* of the small ROIs can vary considerably depending on their placement while the large cortical and parenchyma ROI show very little change based on the plots.

The renal parenchyma mean provides the highest inter-rater agreement (Table 1 and Figure 2). Small ROIs (cortex and medulla) show the least agreement between raters, and the medulla has the lowest inter-rater agreement of all regions (ICC=0.76). When we analyzed the control and CKD groups separately, the ICC values were not significantly different, 0.76 for CKD *vs.* 0.80 for control (other regions not shown). Since the large cortex has a higher level of agreement than the small cortex does, it is the only region assessed outside of the comparison of intra-class correlation.

When comparing baseline and post-furosemide mean R2* values, the parenchyma mean shows a significant difference in control subjects (Table 2a). Subjects with CKD also show a

change in the medulla and the parenchyma ($p < 0.05$), but the magnitude of the change is considerably less than in the control group as indicated by d (Table 2b).

When comparing controls and subjects with CKD at baseline, the cortical ROI shows a significant difference between control and CKD subjects while the parenchyma mean does not (Table 3a). However, after furosemide administration, both regional and parenchyma ROIs show a significant difference, with the parenchyma showing the largest effect size (Table 3b). The cortical effect size decreased from baseline and the medulla also shows a significant difference.

No significant difference was found between left and right kidneys using any of the traditional ROI analysis technique or between any of the moments (data not shown).

Moment Analysis

Figure 3 illustrates a representative distribution of renal parenchymal R2* values at baseline and after administration of furosemide in a control subject. Clearly one can visualize differences in these distributions. Consistent with the mean value, the higher moments of the parenchyma data showed similar trends. Table 5a shows that all four moments are significantly different following furosemide in the control group. While there was no significant difference observed at baseline between CKD and control subjects (Table 6a), post-furosemide show that the first two and the fourth moments are significantly different (Table 6b). Additionally, ICC assessed inter-rater agreement of these moments was comparable to large cortical regions (Table 4).

Discussion

Comparison of Mean Values

Our results demonstrate that the renal parenchyma mean is highly objective in terms of inter-rater reliability and is able to detect intra-subject changes following administration of furosemide, a widely used pharmacological maneuver for BOLD MRI studies. It is well known that the observed changes following furosemide are regional, with the medulla showing a large change in R2* while the cortex shows minimal to no change. Despite not segmenting the medulla, this regional change is still detectable. Whether the same trend will be observed with other pharmacological maneuvers will require further work.

The need for including effect size in order to determine a significant result cannot be understated. Scientific literature has generally placed emphasis on a statistical significance that is based solely on the *p*-value, typically at a significance level of 0.05. However, $p < 0.05$ does not necessarily mean that the observed difference is of any practical consequence. Even small differences will reach statistical significance provided the sample size is large enough[25]. It is considerably more informative to determine an estimate of the magnitude of the difference and whether it is large enough to differentiate a condition of interest, *e.g.* healthy *vs*. CKD. It has been suggested that the effect size should be reported along with, or in place of, p-values[25,27]. Previous reports have suggested that an effect size of 0.5 could be considered a medium effect and 0.8 considered as a large effect. In this report, we have used

$p<0.05$ and $d>0.5$ to imply a pragmatic notion of significance. Further work may be necessary to reach consensus on what value would be optimal for specific applications.

Cortical R2* values were significantly higher in subjects with CKD (Table 3a). While the mean parenchyma R2* values at baseline did not show a difference between the groups, when evaluated post-furosemide, all regions were found to be significantly different. The parenchyma mean actually showed a larger effect size than the cortex at this stage or at baseline. Post-furosemide data combines the differences in cortical R2* values and the responses to furosemide in the medulla between the groups of subjects.

Physiological Interpretation—The mean R2* value (or first moment) of the parenchyma and medulla demonstrated significant changes post-furosemide in control subjects. The observed medullary changes in healthy controls are consistent with several prior reports[7,10,28,29]. The mean R2* value of the parenchyma would be a weighted mean of the cortical and medullary compartments. This results in a smaller effect size (d=0.84) compared to the medulla (d=1.59). However, the ability to detect these changes without regional segmentation indicates that the contributions (magnitude and voxel count) from the medulla are sufficiently large. While the response to furosemide in subjects with CKD also reached p values <0.05, the effect sizes were all quite small, indicating a considerably smaller change in R2*. This trend is consistent with a recent report[10]. The ability to detect differences based on the renal parenchyma without *a priori* knowledge of regional anatomy greatly simplifies image analysis and is expected to be beneficial in comparing data from different institutions.

R2* is used as a surrogate for oxygenation due to its sensitivity to the saturation of hemoglobin (sHb). However, this depends on both oxygen delivered and oxygen consumed. Furosemide provides a method to reduce the local oxygen consumption in the medulla in healthy functioning kidneys and results in a higher blood oxygenation, observed as a decrease in R2*. Prior studies have captured these differences by evaluating ΔR2* following furosemide with significantly lower changes in subjects with CKD[30]. Our results with analyzing post-furosemide R2* distributions of renal parenchyma demonstrate an alternative way of capturing the relative differences in response to furosemide. This is most probably related to the opportunistic leveraging of both the increased cortical R2* in CKD and a lower response to furosemide in the medulla.

The chronic hypoxia model suggests that subjects with progressive CKD may exhibit higher renal hypoxia[31]. Additionally it is estimated that only 1 in 3 patients at stage 3 have progressive CKD[31]. Thus, it is possible that the differences observed between subjects with CKD and healthy controls are smaller than they would be if the group assessed in this study was restricted to just progressors. To-date, no study assessing renal oxygenation has sought to, or identified subjects with progressive CKD.

Multiple Moment Analysis

By looking at higher moments we were able to capture more changes in the shape of the R2* distribution than would be possible with only the mean (Table 5). Figure 3 shows a typical case of how the distributions varied between baseline and post-furosemide in a control

subject. The mean or first moment (μ_1) provides information regarding the central tendency of the distribution. The second moment (μ_2) indicates the spread of the distribution and may be related to the separation of R2* values between the cortical and medullary regions (clearly the spread is lowered post furosemide). The third moment (μ_3) relates to the skewness of the distribution and may indicate the relative strength of each compartment (also lower post-furosemide). Lastly, the fourth moment (μ_4) provides information about the relative magnitude of the tails, the values far from the center of the distribution (clearly this is smaller post-furosemide). However, it is not yet clear how to interpret these additional parameters in practical terms.

There are some limitations with our study. It is important to note that our healthy control group was not age matched to the CKD group. This was primarily due to logistical challenge of recruiting healthy elderly subjects. Earlier reports have failed to demonstrate any significant differences in cortical R2* values with age[10]. However, contributions from age related differences might not be ruled out in our observations. A previous paper did show that response to furosemide might be blunted in older subjects[7], possibly accounting for the difference in post-furosemide R2* values between controls and subjects with CKD observed here. In this preliminary study, the CKD group had a heterogenous distribution of eGFRs, etiologies and medications. Additionally, potential movement between baseline and post-furosemide images may shift the region of the kidney being analyzed.

While the thresholds used for determining significance of our results seem to be appropriate for the context of this work, they will require independent validation to reach consensus.

Use of the renal parenchyma in place of the cortex and medulla has been used in prior reports. Ebrahimi et al modeled the distribution as a two compartment model whose applicability is not strictly feasible when there is limited contrast between cortex and medulla, e.g. subjects with CKD or in healthy subjects post-furosemide[15]. Piskunowicz et al did not assume a two compartment model, but their approach involves the use of a discrete number of layers, each adding several new parameters to the analysis[16]. Saad et al used a measure of fractional tissue hypoxia from the whole parenchyma as a replacement for individual regional measures from the cortex and medulla. This method used a fixed value of 30 sec^{-1} to separate R2* values into high and low levels of hypoxia[14]. Our approach requires no *apriori* assumptions. It may be more straightforward to implement, even though custom software will be necessary. Future consensus from the user community may be necessary for optimal choice among the methods for more general acceptance.

In conclusion, our results show that the mean of the renal parenchyma provides a higher inter-rater agreement when analyzing renal R2* maps than cortical or medullary ROIs. In addition, it shows sufficient sensitivity, in terms of the effect size, when evaluating the response to furosemide, a well-established pharmacologic maneuver in renal BOLD MRI. A new finding is that post-furosemide R2* maps may show more significant differences between controls and subjects with CKD with both a conventional regional ROI analysis and the proposed analysis using the entire renal parenchyma. In addition, by using higher moments, the sensitivity to detecting both inter- and intra-subject differences could be

improved. However, the physiologic interpretation requires further studies and independent validation.

As take home messages, our data support the use of the entire renal parenchyma when analyzing R2* maps from subjects with minimal cortico-medullary contrast. Alternately, large cortical ROIs could be used for evaluating baseline differences between different groups of subjects. Even in healthy subjects, the use of both cortical, and parenchyma analysis may be preferred for comprehensive and objective evaluation. The limitations of using only *p* values for significance have been known, but our data further highlight the need to use additional information such as the effect size.

Acknowledgements

We would like to thank Drs. Huan Tan, Ed Wang and Ioannis Koktzoglou for their scientific input and Mrs. Claire Feczko for editorial support in preparing this manuscript and Mrs. Shonny Fettman for technical assistance during the study.

Grant Support: Work supported in part by grant from the National Institutes of Health, R21-DK079080 and R01-DK093793.

References

1. Nangaku M. Chronic hypoxia and tubulointerstitial injury: a final common pathway to end-stage renal failure. J Am Soc Nephrol. 2006; 17(1):17–25. [PubMed: 16291837]
2. Fine LG, Orphanides C, Norman JT. Progressive renal disease: the chronic hypoxia hypothesis. Kidney Int. 1998:S74–S78.
3. Prasad PV, Edelman RR, Epstein FH. Noninvasive evaluation of intrarenal oxygenation with BOLD MRI. Circulation. 1996; 94(12):3271–3275. [PubMed: 8989140]
4. Li, L-P.; Prasad, PV. Studies on Renal Disorders. Springer; 2011. Estimation of Kidney Oxygenation by Blood Oxygenation Level Dependent Magnetic Resonance Imaging; p. 587-609.
5. Li L-P, Franklin T, Du H, et al. Intrarenal oxygenation by blood oxygenation level-dependent MRI in contrast nephropathy model: effect of the viscosity and dose. J Magn Reson Imaging. 2012; 36(5):1162–1167. [PubMed: 22826125]
6. Li L-P, Ji L, Santos Ea, Dunkle E, Pierchala L, Prasad P. Effect of nitric oxide synthase inhibition on intrarenal oxygenation as evaluated by blood oxygenation level-dependent magnetic resonance imaging. Invest Radiol. 2009; 44(2):67–73. [PubMed: 19034027]
7. Epstein FH, Prasad P. Effects of furosemide on medullary oxygenation in younger and older subjects. Kidney Int. 2000; 57(5):2080–2083. [PubMed: 10792627]
8. Inoue T, Kozawa E, Okada H, et al. Noninvasive evaluation of kidney hypoxia and fibrosis using magnetic resonance imaging. J Am Soc Nephrol. 2011; 22(8):1429–1434. [PubMed: 21757771]
9. Michaely HJ, Metzger L, Haneder S, Hansmann J, Schoenberg SO, Attenberger UI. Renal BOLD-MRI does not reflect renal function in chronic kidney disease. Kidney Int. 2012; 81(7):684–689. [PubMed: 22237750]
10. Pruijm M, Hofmann L, Piskunowicz M, et al. Determinants of renal tissue oxygenation as measured with BOLD-MRI in chronic kidney disease and hypertension in humans. PLoS One. 2014; 9(4):e95895. [PubMed: 24760031]
11. Xin-Long P, Jing-Xia X, Jian-Yu L, Song W, Xin-Kui T. A preliminary study of blood-oxygen-level-dependent MRI in patients with chronic kidney disease. Magn Reson Imaging. 2012; 30(3): 330–335. [PubMed: 22244540]
12. Neugarten J. Renal BOLD-MRI and assessment for renal hypoxia. Kidney Int. 2012; 81(7):613–614. [PubMed: 22419042]
13. Lee VS, Kaur M, Bokacheva L, et al. What causes diminished corticomedullary differentiation in renal insufficiency? J Magn Reson Imaging. 2007; 25(4):790–795. [PubMed: 17335025]

14. Saad A, Crane J. Human Renovascular Disease: Estimating Fractional Tissue Hypoxia to Analyze Blood Oxygen Level – dependent MR. Radiology. 2013; 268(3)
15. Ebrahimi B, Gloviczki M, Woollard JR, Crane JA, Textor SC, Lerman LO. Compartmental Analysis of Renal BOLD MRI Data. Invest Radiol. 2012; 47(3):175–182. [PubMed: 22183077]
16. Piskunowicz M, Hofmann L, Zuercher E, et al. A new technique with high reproducibility to estimate renal oxygenation using BOLD-MRI in chronic kidney disease. Magn Reson Imaging. 2015; 33(3):253–261. [PubMed: 25523609]
17. Lubbers DW, Baumgartl H. Heterogeneities and profiles of oxygen pressure in brain and kidney as examples of the PO2 distribution in the living tissue. Kidney Int. 1997; 51:372–380. [PubMed: 9027709]
18. Tumkur S, Vu A, Li L, Prasad PV. Evaluation of Intrarenal Oxygenation at 3.0 T Using. Invest Radiol. 2006; 41(2):181–184. [PubMed: 16428990]
19. Zhang JL, Morrell GR, Lee VS. Blood oxygen level-dependent MR in renal disease: moving toward clinical utility. Radiology. 2013; 268(3):619–621. [PubMed: 23970506]
20. Valsasina P, Rocca Ma, Agosta F, et al. Mean diffusivity and fractional anisotropy histogram analysis of the cervical cord in MS patients. Neuroimage. 2005; 26(3):822–828. [PubMed: 15955492]
21. Lu S, Ahn D, Johnson G, Law M, Zagzag D, Grossman RI. Radiology Diffusion-Tensor MR Imaging of Intracranial Neoplasia and Associated Peritumoral Edema: Introduction of the Tumor Infiltration Index. Neuroradiology. 2004; 232(4):221–228.
22. Gaing B, Sigmund EE, Huang WC, et al. Subtype Differentiation of Renal Tumors Using Voxel-Based Histogram Analysis of Intravoxel Incoherent Motion Parameters. Invest Radiol. 2014
23. Rossi C, Artunc F, Martirosian P, Schlemmer H-P, Schick F, Boss A. Histogram analysis of renal arterial spin labeling perfusion data reveals differences between volunteers and patients with mild chronic kidney disease. Invest Radiol. 2012; 47(8):490–496. [PubMed: 22766911]
24. Brezis M, Agmon Y, Epstein FH, Brezis M, Agmon Y, Epstein H. Determinants of intrarenal oxygenation. I. Effects of diuretics. Am J Physiol - Ren Physiol. 1994
25. Sullivan GM, Feinn R. Using Effect Size-or Why the P Value Is Not Enough. J Grad Med Educ. 2012; 4(3):279–282. [PubMed: 23997866]
26. Jones E, Oliphant T, Peterson P. SciPy: Open source scientific tools for Python. Available at: http://www.scipy.org/.
27. Greenwald AG, Gonzalez R, Harris RJ, Guthrie D. Effect sizes and p-values: What should be reported and what should be replicated? Psychophysiology. 1996; 33:175–183. [PubMed: 8851245]
28. Li L-P, Prasad P. Evaluation of the Reproducibility of Intrarenal R2* and Delta R2* Measurements Following Administration of Furosemide and During Waterload. J Magn Reson Imaging. 2004; 19(5):610–616. [PubMed: 15112311]
29. Li L-P, Vu AT, Li BSY, Dunkle E, Prasad PV. Evaluation of intrarenal oxygenation by BOLD MRI at 3.0 T. J Magn Reson Imaging. 2004; 20(5):901–904. [PubMed: 15503343]
30. Yin W-J, Liu F, Li X-M, et al. Noninvasive evaluation of renal oxygenation in diabetic nephropathy by BOLD-MRI. Eur J Radiol. 2012; 81(7):1426–1431. [PubMed: 21470811]
31. Fine LG, Norman JT. Chronic hypoxia as a mechanism of progression of chronic kidney diseases: from hypothesis to novel therapeutics. Kidney Int. 2008; 74(7):867–872. [PubMed: 18633339]

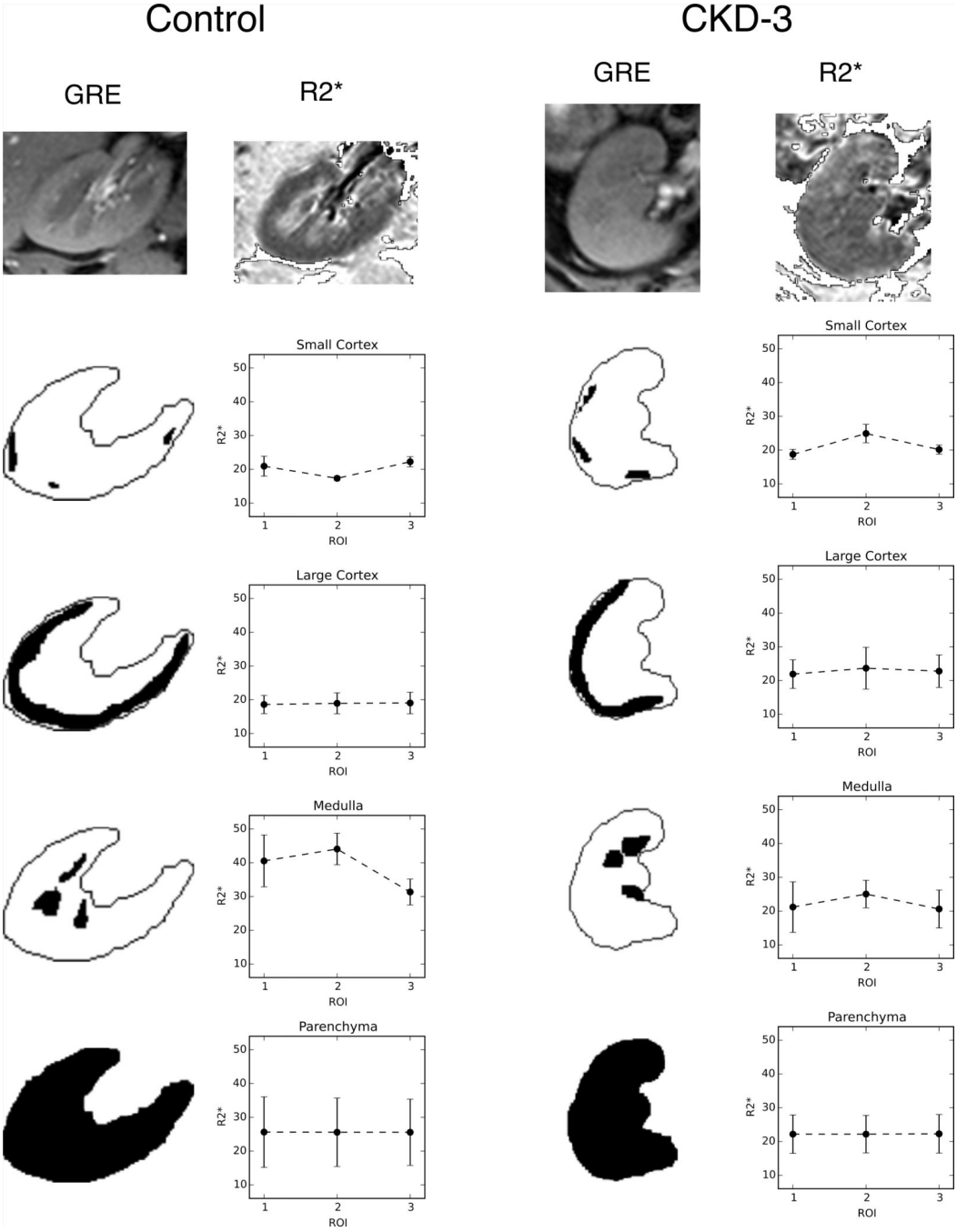

Figure 1.

An example of the variation seen in the mean R2* depending on ROI placement. The left column shows a representative control subject and the right a CKD subject. The first echo from the mGRE images is used as an anatomical template for placing ROIs. The image appears a bit blurry as it is interpolated to this larger size for viewing purposes. The ROI is then used to find the mean of the corresponding region on the calculated R2* map. Three different ROIs are placed for each region (large cortical and parenchyma ROIs are difficult to see due to the overlap of each region). The mean and standard deviations of each region

are shown in the plots. Variation between the ROIs is quite large in the small regions, while the larger ones are clearly not as susceptible to differences in exact placement.

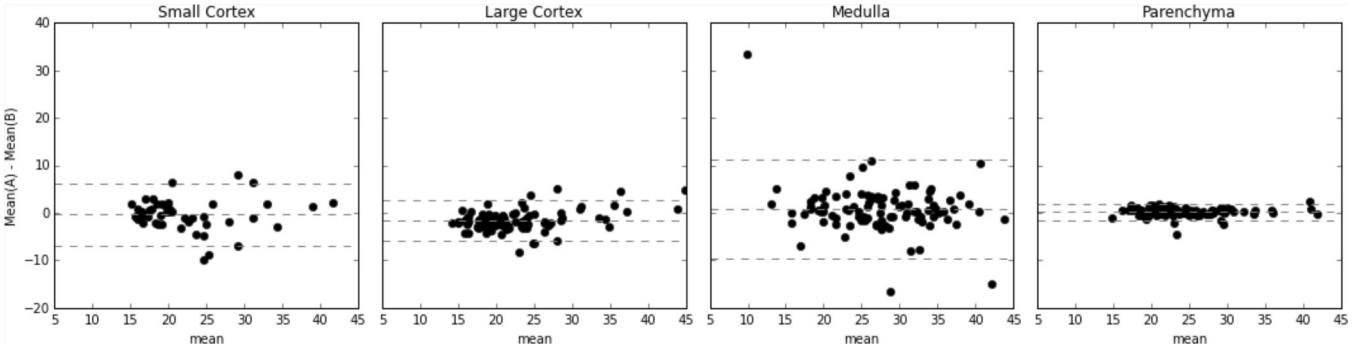

Figure 2.

Mean-difference (Bland-Altman) plots depicting the inter-rater agreement for each ROI region. The medulla shows the highest variation while the parenchyma shows the lowest. Additionally, the large cortex shows a lower level of variation than the small cortex does.

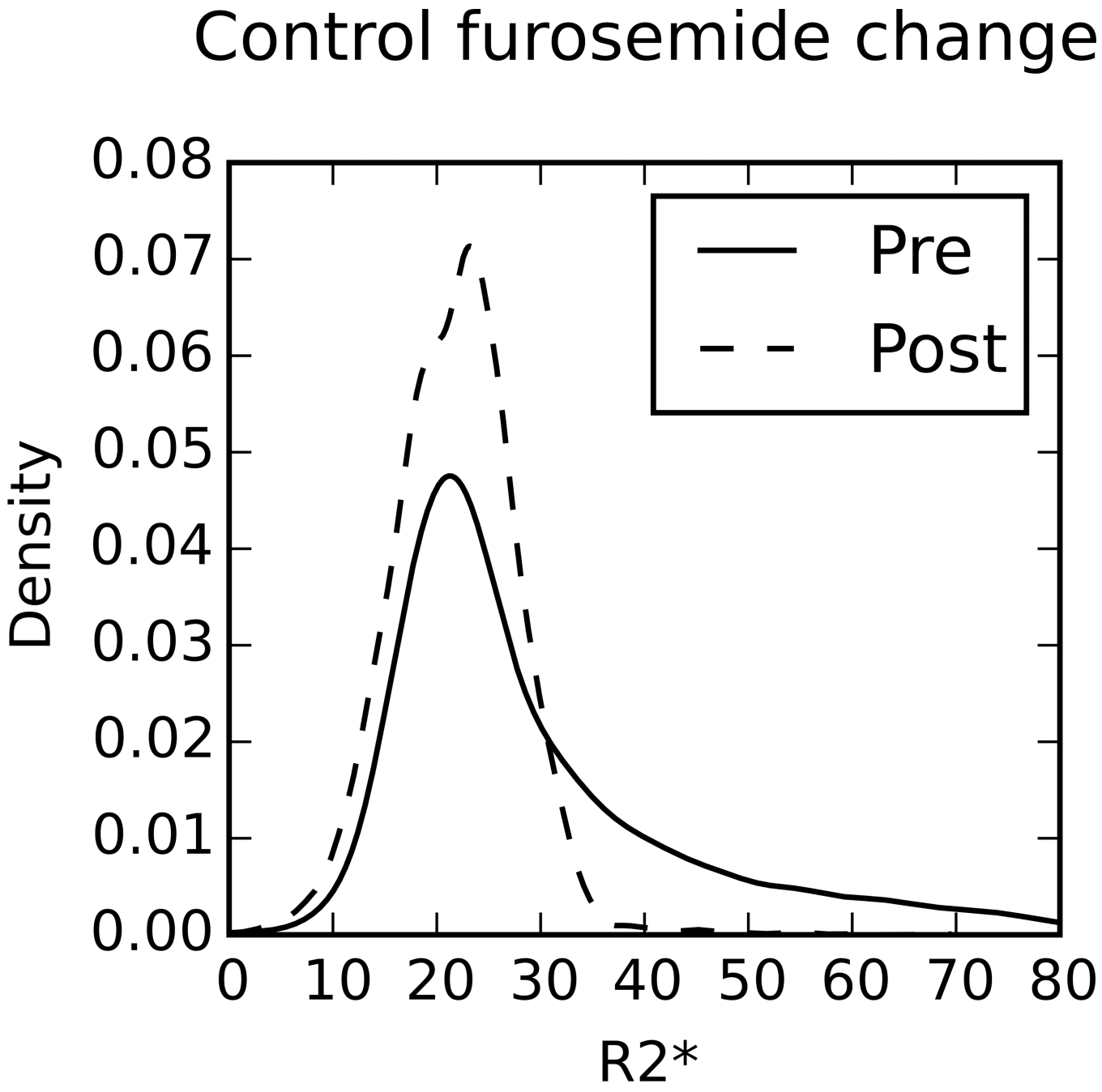

Figure 3.
Example kernel density plots of typical cases for each of the comparisons performed in Tables 3–6. A kernel density plot is used to estimate the empirical distribution and is not sensitive to the bin size like a histogram would be. A kernel density estimate with Gaussian kernels and automatic bandwidth calculation was used to estimate the continuous probability distribution.

Table 1

Intra-class correlation coefficients for mean values of each region at baseline

Region	ICC	95% CI
Small Cortex	0.87	[0.78, 0.92]
Medulla	0.76	[0.61, 0.86]
Large Cortex	0.93	[0.88, 0.96]
Parenchyma	0.99	[0.98, 0.99]

Table 2

a: Controls Baseline vs. Post-furosemide R2*				
Region	**Baseline R2* (s^{-1})**	**Post R2* (s^{-1})**	**P-value †**	**d ‡**
Large Cortex	19.6 ± 3.6	18.7 ± 4.7	0.22	0.21
Medulla	30.9 ± 4.1	22.5 ± 5.0	**0.002**	**1.59**
Parenchyma	23.8 ± 2.7	20.6 ± 4.1	**0.002**	**0.84**

b: CKD Baseline vs. Post-furosemide R2*				
Region	**Baseline R2* (s^{-1})**	**Post R2* (s^{-1})**	**P-value †**	**d ‡**
Large Cortex	23.9 ± 7.3	22.0 ± 6.9	0.056	0.22
Medulla	29.7 ± 7.2	26.7 ± 7.0	0.039	0.35
Parenchyma	26.3 ± 6.1	24.8 ± 5.6	0.004	0.21

† Wilcoxon signed rank test statistic

‡ Cohen's d measure of effect size

Table 3

a: Control vs. CKD at baseline				
Region	**Control R2* (s^{-1})**	**CKD R2* (s^{-1})**	**P-value §**	**d ‡**
Large Cortex	19.6 ± 3.6	23.9 ± 7.3	**0.015**	**−0.69**
Medulla	30.9 ± 4.1	29.7 ± 7.2	0.28	0.18
Parenchyma	23.8 ± 2.7	26.3 ± 6.1	0.152	0.39

b: Control vs. CKD after furosemide				
Region	**Control R2* (s^{-1})**	**CKD R2* (s^{-1})**	**P-value §**	**d ‡**
Large Cortex	18.7 ± 4.7	22.0 ± 6.9	**0.026**	**−0.51**
Medulla	22.5 ± 5.0	26.3 ± 7.0	**0.019**	**−0.61**
Parenchyma	20.6 ± 4.1	24.8 ± 5.6	**0.003**	**−0.75**

§ Mann-Whitney U test statistic

‡ Cohen's d measure of effect size

Table 4

Intra-class correlation coefficients for each of the parenchyma moments

Moment	ICC	95% CI
μ_1	0.99	[0.98, 0.99]
μ_2	0.94	[0.90, 0.97]
μ_3	0.92	[0.86, 0.95]
μ_4	0.90	[0.83, 0.94]

Table 5

a: Higher parenchyma moments: Controls Baseline vs. Post-furosemide				
Shape	**Baseline**	**Post-Furosemide**	**P-value †**	**d ‡**
μ_1	23.8 ± 2.7	20.6 ± 4.1	**0.008**	**0.84**
μ_2	88.7 ± 39	48.5 ± 15	**0.001**	**1.04**
μ_3	$1.26 \pm 0.8 \times 10^3$	$0.59 \pm 0.3 \times 10^3$	**0.007**	**0.83**
μ_4	$53 \pm 43 \times 10^3$	$22 \pm 14 \times 10^3$	**0.007**	**0.72**

b: Higher parenchyma moments: CKD Baseline vs. Post-furosemide				
Shape	**Baseline**	**Post-Furosemide**	**P-value †**	**d ‡**
μ_1	26.3 ± 6.1	24.8 ± 5.6	0.02	0.21
μ_2	79.3 ± 26	73.6 ± 30	0.28	0.17
μ_3	$0.87 \pm 0.53 \times 10^3$	$0.89 \pm 0.65 \times 10^3$	0.56	−0.02
μ_4	$36.5 \pm 22 \times 10^3$	$36.8 \pm 30 \times 10^3$	0.88	−0.01

† Wilcoxon signed rank test statistic

‡ Cohen's d measure of effect size

Table 6

a: Higher parenchyma moments: Baseline Controls vs. CKD				
Shape	**Control**	**CKD**	**P-value** §	**d** ‡
μ_1	23.8 ± 2.7	26.3 ± 6.1	0.30	−0.49
μ_2	88.7 ± 39	79.3 ± 26	0.28	0.23
μ_3	1.3 ± 0.8 $\times 10^3$	0.87 ± 0.5 $\times 10^3$	0.11	0.45
μ_4	53.4 ± 43 $\times 10^3$	36.5 ± 22.4 $\times 10^3$	0.24	0.38

b: Higher parenchyma moments: Post-Furosemide Controls vs. CKD				
Shape	**Control**	**CKD**	**P-value** §	**d** ‡
μ_1	20.6 ± 4.1	24.8 ± 5.7	**0.003**	**−0.75**
μ_2	48.5 ± 15	73.6 ± 30	**0.005**	**−1.00**
μ_3	0.59 ± 0.3 $\times 10^3$	0.89 ± 0.7 $\times 10^3$	0.11	−0.54
μ_4	22.4 ± 14 $\times 10^3$	36.8 ± 29 $\times 10^3$	**0.01**	**−0.59**

§ Mann-Whitney U test statistic

‡ Cohen's d measure of effect size